NUMERICAL METHODS FOR THE VALUATION OF ACCUMULATORS UNDER LOCAL VOLATILITY

FABIEN LE FLOC'H

Abstract. Under the local volatility model, the convergence of Monte-Carlo with Milstein discretization and Euler discretization are compared for the pricing of Vanilla, Digital, discrete Barrier options as well as a more exotic variety of option, the Accumulator. A finite difference approach is also studied. Parametric and Non-Parametric local volatility models are examined.

1. Introduction

The simplest approximation for the simulation of a stochastic differential equation is the Euler scheme [Glasserman, 2003]. Because, under the Black-Scholes assumptions, the asset price follows a lognormal distribution, the Euler scheme is often applied to a log-transformed variable and not directly to the asset price for financial problems. We will look at the impact of this transformation on the convergence when the asset price does not follow a log-normal distribution.

One popular improvement is the Milstein discretization [Glasserman, 2003; Jäckel, 2002; Clark, 2011], of strong order-1 convergence, while Euler is only weak order-1 convergence and strong order-1/2 convergence. A discretization $\hat{X}$ is said of strong order-β convergence if:

$$\mathbb{E}[\|\hat{X}(nh) - X(T)\|] \leq ch^{\beta} \tag{1}$$

for some constant c and all sufficiently small h with $n = \frac{T}{h}$. The discretization scheme is of weak order-β convergence if:

$$|\mathbb{E}[f(\hat{X}(nh))] - \mathbb{E}[f(X(T))]| \leq ch^{\beta} \tag{2}$$

for all f whose derivatives of order 0, 1, ..., $2\beta + 2$ are polynomially bounded. It appears, then, that strong convergence could be of interest for (strongly) path dependent products, as well as to better describe the diffusion. We will study the convergence of Milstein and Euler schemes under a local volatility setting, starting with vanilla options under a simple local volatility model, the displaced diffusion [Rubinstein, 1983], extending to exotic payoffs under a realistic Dupire local volatility [Dupire, 1994]. We will propose some payoff specific performance improvements applicable to the Accumulator. And finally we will study an alternative method of pricing the Accumulator under local volatility, using a partial differential equation approach.

2. The Accumulator

The simplified term-sheet given in Table 1 represents a typical Accumulator deal: a number of shares accrues every day. Double the amount of shares accrues if the asset price is higher than a fixed strike price. This number of accumulated shares

Date: January 25, 2013.

Key words and phrases. Option, Finance, Local Volatility, Monte-Carlo, Milstein, Euler, Accumulator, Displaced Diffusion.

Discussions and exchange of ideas with Gary Kennedy were particularly important.

TABLE 1. Accumulator simplified term-sheet

Start Date	Sep 01 2010
Maturity Date	Sep 01 2011 unless Knock-Out Event happens
Settlement	At each Observation Period end date
Observation Period	Every 30 days between Start Date and End Date
Accumulated Delivery Amount	Total No. of Shares in each observation period
Reference Price	2016
Strike	90% of Reference Price
Daily Delivery Amount	1,200 shares for no. of days during each observation period where closing price of reference security is higher than Forward Price. 600 shares for no. of days during each observation period where closing price is less than Forward Price
Knockout Event Date	During Knockout observation Period, closing price of the reference security is higher than Knockout Price; this deal will terminate and will settle 4 business days after the Knockout event date
Knock Out Observation Period	every day from Start Date to Maturity Date
Knock Out Price	110% of Reference Price

is paid regularly, here monthly. In addition, the whole structure can knock-out if the share price is over a fixed knock-out level. There are several variations around the Accumulator: the accumulated shares can be paid at the knock-out date with an eventual payment lag (we will refer to this as version A), or it can be paid at the corresponding observation period end date (version B). This small difference in characteristics has big consequences. The version B can be replicated by a sum of discrete barrier options [Lam et al., 2009], while version A can not. We will focus here on version A, although all the presented techniques can also be applied to version B. One common extension to the Accumulator is the addition of a TARN feature: the deal will knock-out if the total number of accumulated shares over the period of the deal is higher than a given threshold.

The buyer of such a contract will win if the asset stays between the strike price and the knock-out barrier. It is sometimes referred to as "I kill you later" contract [Santini, 2009]: the losses don't stop until maturity when the asset goes down. For example the price of an Accumulator option corresponding to Table 1 is 4.19 millions for a maturity of 1 year, but becomes -19.25 millions for a maturity of 2 years under displaced diffusion. A related deal is the Decumulator where shares are sold instead of being delivered, the strike is usually higher than the spot, and the knock-out barrier is down instead of up.

We will note S the simulated asset, K the strike, B the knock-out barrier level, Q the total number of accumulated shares and V the option value.

LISTING 1. Forward evaluation pseudo-code

```
AccrualDates:
  if not knockedOut then
    q = S > K? 1200 : 600
    Q = Q + q
  endif
```

```
KnockoutDates:
  if not knockedOut and S >= B then
    Value = Value + Q*(S–K)
    knockedOut = true
 endif

PaymentDates:
   if not knockedOut then
     Value = Value + Q*(S–K)
     Q = 0
   endif
```

Using Monte-Carlo simulation, the Accumulator is priced the following way: inside the Monte-Carlo loop, the forward evaluation pseudo-code in Listing 1 is executed on each generated path. In our numerical examples, we will use Sobol low discrepancy sequence initialized using Joe-Kuo direction numbers [Joe and Kuo, 2008], as well as the Brownian-Bridge variance reduction technique [Glasserman, 2003; Jäckel, 2002].

We will analyze the convergence of a rarely sampled accumulator, where shares accrue every 15 days, and knock-out happens every 15 days (bimonthly), as well as the daily accumulator.

3. Milstein Discretization of the Local Volatility model

We consider one dimensional processes S satisfying the following stochastic differential equation:

$$\frac{dS(t)}{S(t)} = \mu(S,t)dt + \sigma(S,t)dW(t) \tag{3}$$

3.1. Direct Discretization.

The Euler time-discretization $\hat{S}$ is defined by Glasserman [2003]:

$$\hat{S}_{i+1} = \hat{S}_i + \mu(\hat{S}_i, t_i)\hat{S}_i\Delta t_i + \sigma(\hat{S}_i, t_i)\hat{S}_i\sqrt{\Delta t_i}Z_i \tag{4}$$

where $Z_0, Z_1, ...$ are independent standard normal random numbers and $\Delta t_i = t_{i+1} - t_i$. The Milstein time-discretization is usually obtained for μ and σ that depend only on S and not on the time t directly. Like Clark [2011], we extend the Milstein discretization to our more general and practical time-dependent μ and σ:

$$\hat{S}_{i+1} = \hat{S}_i + \mu(\hat{S}_i, t_i)\hat{S}_i\Delta t_i + \sigma(\hat{S}_i, t_i)\hat{S}_i\sqrt{\Delta t_i}Z_i \tag{5}$$

$$+ \frac{1}{2}\sigma(\hat{S}_i, t_i)\hat{S}_i\left(\hat{S}_i\frac{\partial\sigma}{\partial S}(\hat{S}_i, t_i) + \sigma(\hat{S}_i, t_i)\right)(Z_i^2 - 1)\Delta t_i \tag{6}$$

3.2. Lognormal Discretization.

When μ and σ are constant, that is when the process S is a geometrical Brownian motion, the Euler discretization of the log process $X = ln(S)$ is then exact as we have $\hat{X}_i = X(t_i)$. Furthermore the discretized process will naturally respect the condition $S > 0$. It appears, then, that the log transformation has much to commend. However, in practice, the advantages are not so dramatic, as μ and σ^2 are relatively small and Δt_i is likely to be smaller than 1. The log transform is also more costly due to the need of calling the exponential function inside the Monte-Carlo loop. The Log-Euler time-discretization follows from the application of Ito:

$$\hat{X}_{i+1} = \hat{X}_i + \left(\mu(\hat{X}_i, t_i)) - \frac{1}{2}\sigma^2(\hat{X}_i, t_i)\right)\Delta t_i + \sigma(\hat{X}_i, t_i)\sqrt{\Delta t_i}Z_i \tag{7}$$

And the Log-Milstein time-discretization is:

$$\hat{X}_{i+1} = \hat{X}_i + \left(\mu(\hat{X}_i, t_i) - \frac{1}{2}\sigma^2(\hat{X}_i, t_i)\right)\Delta t_i + \sigma(\hat{X}_i, t_i)\sqrt{\Delta t_i} Z_i \tag{8}$$

$$+ \frac{1}{2}\sigma(\hat{X}_i, t_i)\frac{\partial \sigma}{\partial X}(\hat{X}_i, t_i)(Z_i^2 - 1)\Delta t_i \tag{9}$$

The two schemes are equivalent when the volatility σ is constant.

3.3. **Improvements.** In practice, the drift is state independent, and we can use the effective drift $\hat{\mu}$ defined by Clark [2011]:

$$\hat{\mu}(X_i, t_i) = \int_{t_i}^{t_{i+1}} \mu(t) dt \tag{10}$$

Thus $\hat{\mu}$ can be directly computed from the discount factors. Using the effective drift will make the Monte-Carlo simulation price correctly a forward contract, even with a large time-step, when the drift is not constant. This idea of using an effective drift instead of the instantaneous drift in order to correctly price the forward is also presented in [Andersen and Brotherton-Ratcliffe, 1998] in the context of PDE discretization. Clark also proposes a better estimate of the local volatility used in the discretization than using the instantaneous local volatility directly:

$$\hat{\sigma}^2(X_i, t_i) = \frac{1}{2}\left(\sigma^2(X_i, t_i) + \sigma^2(\mathbb{E}[X(t_{i+1})|F_{t_i}], t_{i+1})\right) \tag{11}$$

where a simple estimate is for the log schemes:

$$\mathbb{E}[X(t_{i+1})|F_{t_i}] = \hat{X}_i + \left(\hat{\mu}(\hat{X}_i, t_i) - \frac{1}{2}\hat{\sigma}^2(\hat{X}_i, t_i)\right)\Delta t_i \tag{12}$$

And for the standard discretizations:

$$\mathbb{E}[S(t_{i+1})|F_{t_i}] = \hat{S}_i + \hat{\mu}(\hat{S}_i, t_i)\Delta t_i \tag{13}$$

4. Predictor-Corrector Discretization of the Local Volatility

The predictor-corrector method takes explicitely into account the time-varying and path-varying nature of the drift and volatility [Jäckel, 2002]. The predictor step is the classic Euler discretization $\hat{S}_i$ given by equation 4. The corrector uses two weights θ and η usually set to $\frac{1}{2}$:

$$\overline{S}_{i+1} = \overline{S}_i + \left(\theta a_{i+1}(\hat{S}_{i+1}) + (1-\theta)a_i(\overline{S}_i)\right)\Delta t_i \tag{14}$$

$$+ \left(\eta b_{i+1}(\hat{S}_{i+1} + (1-\eta)b_i(\overline{S}_i)\right)\sqrt{\Delta t_i} Z_i \tag{15}$$

where

$$a_i(S) = \mu(S, t_i) - \eta b_i \frac{\partial b_i}{\partial S}(S, t_i) \tag{16}$$

$$b_i(S) = \sigma(S, t_i) S \tag{17}$$

Contrary to the Milstein scheme, the predictor-corrector method can be extended to N correlated processes in a straightforward manner. Like the Euler scheme, it is of weak order-1 and of strong order-1/2. It will require more computational power in order to lookup the local volatility at $\hat{S}_{i+1}$ as well as its derivative. In our tests, it can be up to twice slower as the basic Euler discretization when the number of time-steps is large.

5. Displaced Diffusion

The displaced diffusion model [Rubinstein, 1983] is a very simple local volatility model, with a parametric volatility function of S only. It has two important properties: the availability of closed formulas for the price of vanilla options, and it is a first approximation to any local volatility smile near the money [Andersen and Piterbarg, 2010, p. 286]. As it is not time-dependent, it could be seen as the ideal candidate for Milstein discretization.

For simplicity, we study the case with no drift. This lets us focus on the effect of the volatility smile and shortens the equations. Under the displaced diffusion model, the asset follows under the risk neutral measure $\mathbb{Q}$:

$$dS(t) = (\beta S(t) + (1-\beta)S(0))\,\sigma dW(t) \tag{18}$$

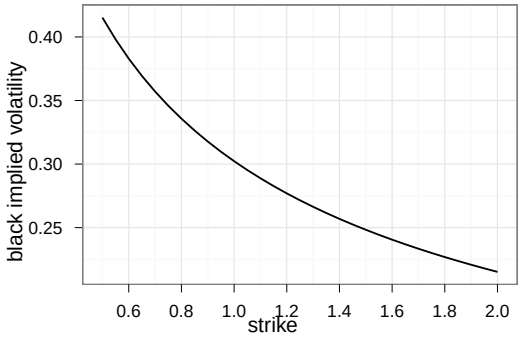

Figure 1. Implied volatility smile for a displaced diffusion with $S(0) = 1$, $T = 2.0$ years, $\sigma = 30\%$, $\beta = \frac{1}{16}$

Let $R(t) = S(t) + \frac{1-\beta}{\beta}S(0)$, we have

$$dR(t) = \beta R(t)\sigma dW(t)$$

As R is a lognormal process, it is well known that

$$R(t) = R(0)e^{-\frac{1}{2}\sigma^2\beta^2 t + \sigma\beta W(t)}$$

Therefore

$$S(t) = \frac{1}{\beta}S(0)e^{-\frac{1}{2}\sigma^2\beta^2 t + \sigma\beta W_S(t)} - \frac{1-\beta}{\beta}S(0) \tag{19}$$

From Equation 19 we deduce that the price of a vanilla call option can be obtained with the standard Black-Scholes formula applied to a shifted strike $K + \frac{1-\beta}{\beta}S(0)$, an initial spot of $\frac{1}{\beta}S(0)$, and a volatility of $\sigma\beta$ when $\beta \neq 0$.

5.1. Normal vs Log-Normal distribution.

When $\beta = 0$ the displaced diffusion has a normal distribution, when $\beta = 1$ it has a log-normal distribution. This allows us to easily look at the implications of the underlying distribution on the discretization scheme. We use $S(0) = 2016$, $\mu = 0\%$ and time to expiry $T = 1$. As expected, under a log-normal distribution, log-Euler and log-Milstein are equivalent, and are the best schemes (Figure 2). The simple Euler fares relatively poorly, while Milstein can have as good convergence as the log discretizations when the number of time-steps increases. The results are similar on out-of-the-money and in-the-money vanilla options, with Milstein outperforming Euler more significantly.

FIGURE 2. Call option price convergence with different time-steps with S following a lognormal distribution. ITM, OTM, ATM respectively stand for options with strikes 80%, 120%, 100%.

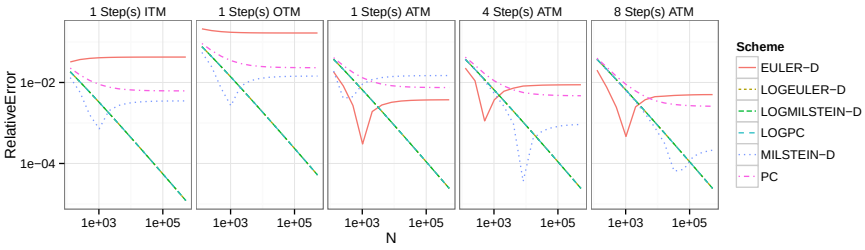

FIGURE 3. At-the-money vanilla call option price convergence with different time-steps with S following a normal distribution

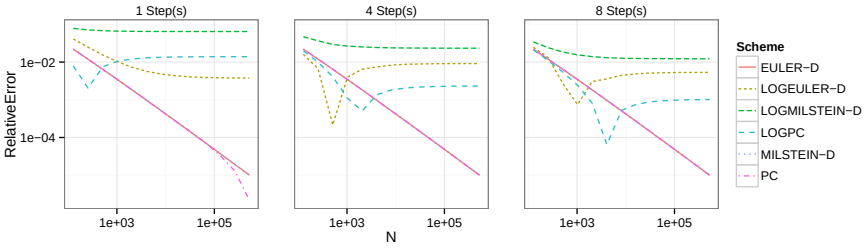

Similarly, under normal distribution, Euler and Milstein are equivalent, and are the best schemes (Figure 3). The graphs of out-of-the money or in-the-money options are similar but with log-Milstein converging slightly better than log-Euler. The log-Milstein scheme has a suprisingly poor convergence, close to the one of log-Euler, even when the number of time-steps increases. This is likely because the log-discretization imposes $S > 0$ while under a normal distribution, S can be negative with positive probability.

5.2. **Vanilla Convergence.** In the following numerical studies, we use $\beta = \frac{1}{2}$ so that we are in effect in between the normal and the lognormal modes.

The reference price is obtain by the closed formed formula implied by Equation 19. Figure 4 presents the relative error evolution as a function of the number of

FIGURE 4. Call option price convergence with different time-steps. ITM, OTM, ATM respectively stand for options with strikes 80%, 120%, 100%.

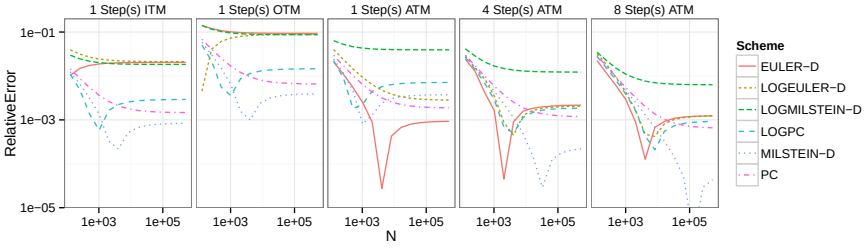

Monte-Carlo paths, for various time-steps. The standard Milstein scheme strongly outperforms the other schemes, especially when the number of time-steps increases. Interestingly, the log-Milstein scheme is worse than the log-Euler scheme.

FIGURE 5. vanilla call option price convergence with 1 time-step - Iain Clark correction. ITM, OTM, ATM respectively stand for options with strikes 80%, 120%, 100%.

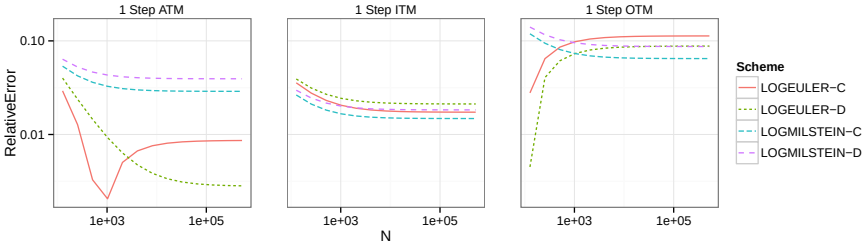

The Clark correction does not offer a convincing improvement in convergence in this case (schemes ending with -C in Figure 5), this is likely because the displaced diffusion is constant over time, the Clark correction only impacts the log-schemes.

5.3. **Digital Convergence.** A digital option can be seen as a limit of call spread [Taleb, 1997, p. 281]:

$$DC(K) = \frac{1}{\epsilon}(C(K) - C(K+\epsilon)) \tag{20}$$

where $DC(K)$ is the price of a digital call option of strike K and $C(K)$ is the price of a vanilla option of strike K. This is how we find the reference value of our example option. In contrast, the popular closed formed formula found in [Haug, 2006] don't take the smile into account.

FIGURE 6. Digital call option price convergence with different time-steps.ITM, OTM, ATM respectively stand for options with strikes 80%, 120%, 100%.

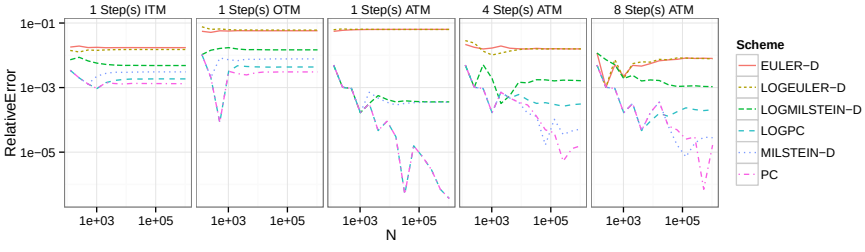

The Milstein and the Predictor-Corrector have best convergence (Figure 6). The Euler and log-Euler convergence graphs are nearly flat with regard to the number of simulations, the log-Milstein convergence is in between the Euler and Milstein convergence.

5.4. **Discrete Barrier Convergence.** Let's look at a discrete barrier option, at-the-money. We obtain a very accurate price by finite difference using the TR-BDF2 scheme [Le Floc'h, 2013], placing the barrier points in the middle of the grid, with a fine grid of 1000 time steps and 4000 space steps. We consider an up-and-out barrier at 120% of the spot level, discretely monitored, with monitoring every 182 days (nearly 6 months), and monitoring every 30 days (nearly 1 month). The Monte-Carlo simulation will proceed in a minimum of respectively 3 (2 barrier dates and 1 maturity) and 13 time-steps.

FIGURE 7. Discrete up-and-out price convergence per number of time-steps and knock-out dates

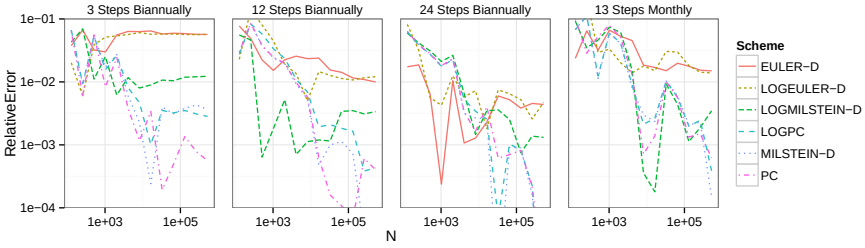

Both Milstein and log-Milstein schemes have much better convergence than Euler or log-Euler for a discretely monitored up-and-out call (Figure 7). When the number of time-steps increases, be it due to the number of knock-out dates or to a choice of discretization, the Milstein scheme convergence is closer to that of the other schemes, but still offers a good improvement for up to 24 time-steps.

FIGURE 8. Discrete down-and-out price convergence per number of time-step and knock-out dates

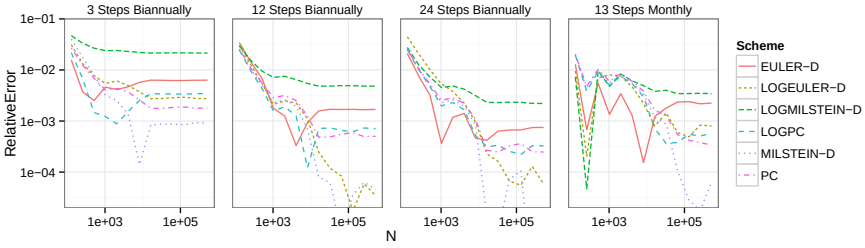

The log-Milstein scheme has, however, the worst convergence on an down-and-out call (Figure 8), while the standard Milstein scheme maintains its outperforming convergence. Overall, the Milstein scheme has the best convergence on discrete barrier problems.

5.5. **Accumulator.** We study now the case of a more exotic payoff, particularly popular in Asia, the Accumulator option.

Milstein and Predictor-Corrector offer a good improvement in convergence for the bimonthly Accumulator (24 time-steps). For the daily accumulator, the minimum number of evaluation dates here is one per day, as shares accrue every day. As expected, on the daily accumulator, Milstein discretization does not offer any improvement over Euler, because the time-step is small enough so that the Milstein

FIGURE 9. Accumulator option price convergence

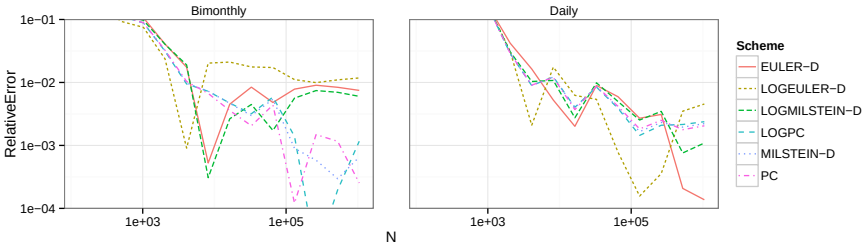

discretization additional term is neglectible. In our tests, using the Java language on the latest JVM 1.7, the Euler scheme is up to 40% faster than the log-Euler one. The difference can be directly attributed to the exponential function overhead.

5.6. **Summary of Displaced Diffusion convergence tests.** The log-Milstein and standard Milstein schemes perform very differently. Milstein converges much faster than Euler or log-Euler, while log-Milstein has often the worst convergence. There is however little difference in the convergence of log-Euler compared to Euler as long as the distribution is not purely normal or purely lognormal, the same had been noticed in the case of Libor Market Model simulation in [Andersen and Andreasen, 2000].

The predictor-corrector also allows to gain precision significantly, usually by an order of magnitude, but its convergence is not as good as Milstein for a low number of time-steps. On more realistic exotics, like discrete barriers or the accumulator, it does as well as Milstein, but it is more computationally intensive. The log version of the predictor corrector has only slightly worse convergence.

6. DUPIRE LOCAL VOLATILITY

The Dupire local volatility model is often used in practice, as it can reproduce the smile very accurately [Dupire, 1994]. The local volatility σ is given as a function of the market vanilla option implied variances by [Gatheral, 2006]:

$$\sigma^2(y,t) = \frac{\frac{\partial w}{\partial t}}{1 - \frac{y}{w}\frac{\partial w}{\partial y} + \frac{1}{4}\left(-\frac{1}{4} - \frac{1}{w} + \frac{y^2}{w^2}\right)\left(\frac{\partial w}{\partial y}\right)^2 + \frac{1}{2}\frac{\partial^2 w}{\partial y^2}} \tag{21}$$

with $y = \log(\frac{K}{F})$, K a vanilla option strike, F the forward price at time t, $w(y,t)$ the total implied variance of the option of maturity t and moneyness y.

We consider Gatheral SVI parameterization of the implied volatility surface in order to have a smooth surface. This is especially important as the Dupire formula relies on the second derivatives of the price over the strike, or on the second derivative of the implied variance over the log-moneyness when expressed as in Equation 21. For a given slice of maturity t, the parameterization is:

$$w(y,t) = at + bt\left[\rho(y-m) + \sqrt{(y-m)^2 + \omega^2}\right] \tag{22}$$

with a, b, ρ, m, ω obtained by best fitting to market prices. The implied volatility is interpolated in time using a linear interpolation in variance along constant log-moneyness.

In the Monte-Carlo simulation, most of the time is spent computing the local volatility. In order to improve significantly the performance of the Monte-Carlo simulation, we use a spline interpolation of the SVI slice in the strike dimension,

FIGURE 10. SVI surface for the Nikkei index on September 17 2010

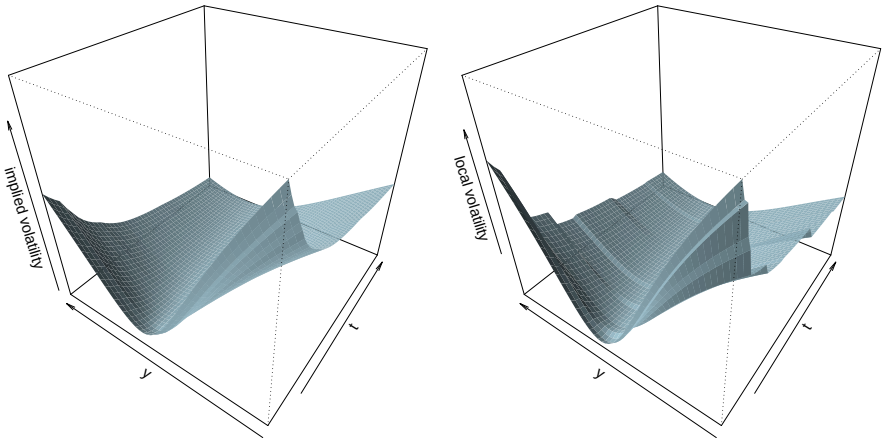

(A) Implied Volatility (B) Local Volatility

and a linear interpolation in the time dimension, using a grid fine enough so as not to loose too much accuracy.

The Dupire model can directly give a discrete approximation to the local volatility between two dates, if one just uses the period length in the Dupire formula discretization. Clark approximation is more relevant than in the displaced diffusion case, because the local volatility varies with time. We compare the effectiveness of the discrete Dupire approach to Clark approximation.

FIGURE 11. Call option of maturity 1 year convergence with different time-steps. ITM, OTM, ATM respectively stand for options with strikes 80%, 120%, 100%.

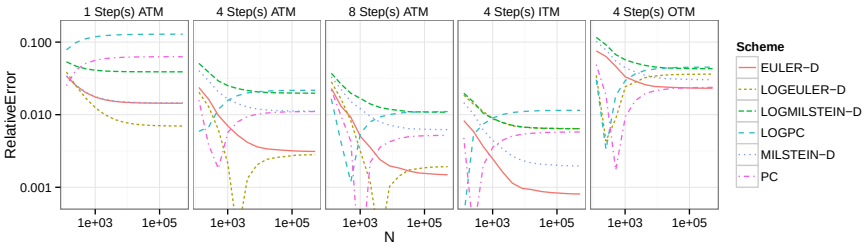

6.1. **Vanilla Convergence.** On an at-the-money option, the log-Euler scheme has best convergence (Figure 11) for a single time-step. The Milstein scheme has almost as good convergence. Like in the displaced diffusion scenario, the log-Milstein scheme has the worst convergence for a vanilla at-the-money call price. Interestingly the basic Euler discretization outperforms every other discretization when the number of time-steps increases, and it always outperforms Milstein. This is however highly dependent on the maturity of our option, when using a shorter maturity, 6 months, the Milstein improvements are more visible and the results are closer to the displaced diffusion case. When the option is in-the-money, the log-Euler scheme is the worst performer. Standard Milstein and Euler have similar convergence and

outperforms the log discretizations. Contrary to the Displaced Diffusion example, Milstein discretization is not particularly attractive compared to Euler in our real world scenario. And the log discretizations, while the most often used, have worse convergence.

FIGURE 12. vanilla call option price convergence with 1 time-step - Iain Clark correction. ITM, OTM, ATM respectively stand for options with strikes 80%, 120%, 100%.

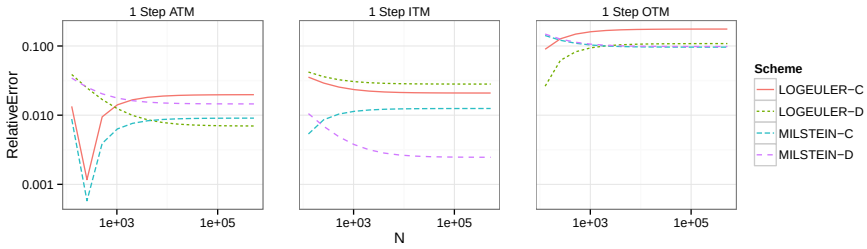

Clark correction does not offer any convincing improvement in the convergence over the discrete Dupire local volatility as can be seen on Figure 12. This can be expected as Clark correction is just a way to estimate the discrete local volatility from the instantaneous local volality, but in our case, we have a direct access to a better estimate via the discrete Dupire local volatility.

FIGURE 13. Digital call option with a maturity of 2 years. ITM, OTM, ATM respectively stand for options with strikes 80%, 120%, 100%

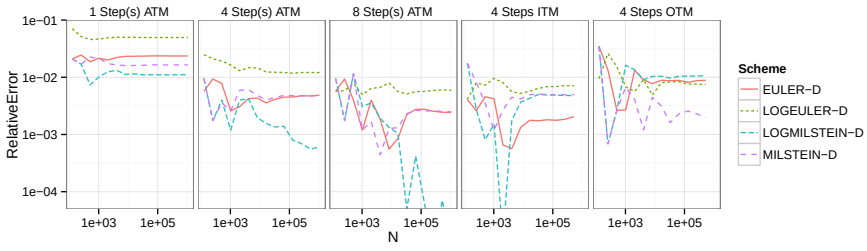

6.2. **Digital Convergence.** Regarding the digital option, the results are similar to the vanilla case when the option maturity is of 1 year. When the maturity is of 2 years, the log-Milstein scheme outperforms the other schemes at-the-money, but not in-the-money or out-of-the-money where all schemes show similar convergence. Log-Euler has the worst convergence overall (Figure 13).

6.3. **Discrete Barrier Convergence.** Simple Euler has also the best convergence among the discretization schemes on a discrete barrier. The log-Milstein scheme has the worst convergence overall (Figures 14 and 15).

FIGURE 14. Discrete up-and-out price convergence per number of knock-out dates and time-steps

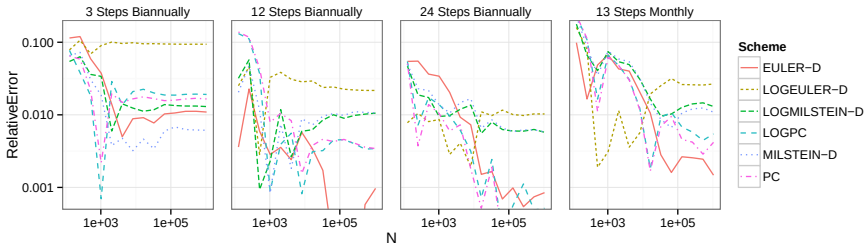

FIGURE 15. Discrete down-and-out price convergence per number of knock-out dates and time-steps

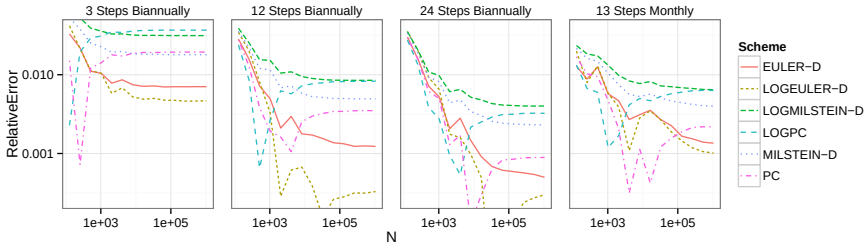

FIGURE 16. Accumulator option price convergence

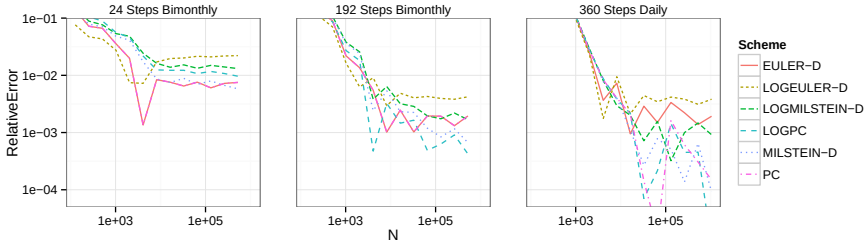

6.4. **Accumulator.** We consider the same deals as in the displaced diffusion Accumulator option example. All the schemes have similar convergence on the bimonthly accumulator: the overall error is high compared to the daily accumulator. 24 time-steps is not enough to capture the diffusion in an fine way. Surprisingly Milstein and the Predictor-Corrector schemes improve the accuracy by an order of magnitude on the daily accumulator when compared to Euler or log-Euler (see Figure 16). The results are similar if the barrier is down at 90% as well as with shorter or longer maturities.

7. Payoff Specific Enhancements

In the case of a daily evaluated discrete barrier, it is possible to avoid the cost of the simulation at every single date by shifting the barrier slightly. This has been proposed in [Gobet, 2008; Andersen and Piterbarg, 2010] relying on the technique to move from a continuous barrier option price to a discrete barrier option price as

described in [Broadie et al., 1997] and more completely in [Kou, 2003]:

$$V_m(B) = V(Be^{\pm\beta\sigma\sqrt{T/m}}) + o(1/\sqrt{m}) \tag{23}$$

where $V_m(B)$ is the price of a discrete barrier option with m monitoring points of maturity T, and $V(B)$ is the price of a continuously monitored barrier option with barrier level B and $\beta \approx 0.5826$.

As shown in [Gobet, 2008], it can be extended to a generic payoff and local or stochastic volatility model, using a more refined approximation when the barrier is near the money by replacing the barrier level B in check $\hat{X}_{i+1} \geq B$ with:

$$\hat{X}_{i+1} \geq Be^{\pm\sigma(\hat{X}_i,t_i)(\beta_m\sqrt{\Delta t_m}-\beta_n\sqrt{\Delta t_n})} \tag{24}$$

to adjust the price from a discretization of step Δt_n to a discretization of step Δt_m where $\beta_m = \bar{y}(\frac{1}{\sigma(X_0,t_0)\sqrt{\Delta t_m}}\log\frac{B}{X_0})$ and $\bar{y}(u) \approx 0.5826 + 0.1245e^{-2.7u^{1.2}}$. $\pm$ is $+$ for an up barrier and $-$ otherwise.

When the discretization is not log-transformed, this can be adjusted to simply:

$$\hat{X}_{i+1} \geq B\left(1 \pm \sigma(\hat{X}_i, t_i)(\beta_m\sqrt{\Delta t_m} - \beta_n\sqrt{\Delta t_n})\right) \tag{25}$$

This kind of approximation supposes that the barrier dates are almost uniformly distributed. Furthermore, the Monte-Carlo engine needs to be aware of the barrier levels in order to shift them. We will now look at the precision given by the adjustment of Equation 25 in practice.

7.1. **Barrier Shifting under Displaced Diffusion.** We consider an at-the-money vanilla option with a daily barrier placed at respectively 120% and 80% of the spot $S(0) = 2016$ with maturity 1-year under displaced diffusion with $\beta = 0.5$, $\sigma = 30\%$ and no drift. The Barrier shifting adjustment allows to reduce the up-and-out barrier price relative error from 10% to 1% (Figure 17) with 1/4 of the original number of evaluation dates. Overall it allows to price 60% faster but at a significant loss of precision. The error becomes really too high for practical use on 22 evaluation dates (1/16 of the original number of dates). The barrier adjustment seems more precise

FIGURE 17. daily barrier option with 512K paths under displaced diffusion. The -S suffix denotes the simulations with shifted barrier.

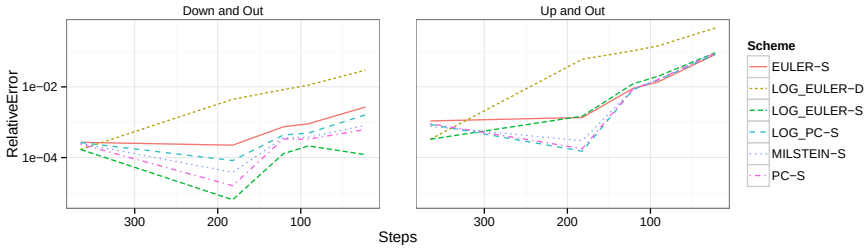

on a down-and-out barrier option. This is because the option is knocked-out in the money. The barrier adjustment allow here to easily divide the computation time by 2 without sacrificing too much accuracy. The different discretization schemes result in a similar error, with Euler being overall slightly less precise.

FIGURE 18. daily barrier option with 512K paths under Dupire Local Volatility. The -S suffix denotes the simulations with shifted barrier.

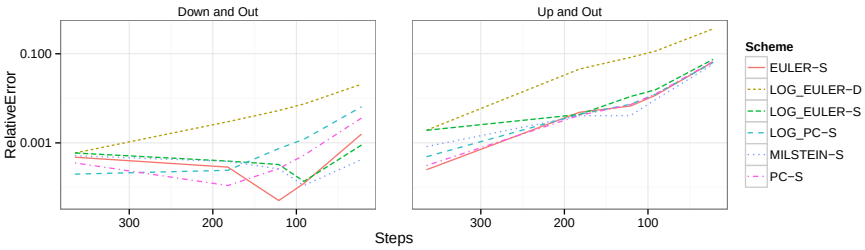

7.2. **Barrier Shifting under Dupire Local Volatility.** We now look at the same options under the Dupire local volatility model based on the volatiltiy surface from Figure 10. It is interesting to compare Figure 18 with Figure 17: the errors are not higher with our realistic volatility surface. The barrier adjustment works as well as under the simpler displaced diffusion model in practice.

Again, the different discretization schemes result in a similar error, with Milstein discretization having slightly lower error overall.

7.3. **Barrier Shifting and the Accumulator.** We consider the same daily Accumulator as described in Table 1 under Dupire local volatility. Because shares accrue every day, we still need to evaluate the Accumulator pseudo-code every day. For the dates that are not part of the simulated path, we simply reuse the path value at the closest previous simulated date, in a piecewise constant interpolation manner. One could think of interpolating linearly the path, but in our experience, it proves to be less accurate.

TABLE 2. Daily Accumulator under Dupire local volatility. The -S suffix denotes the barrier adjusted schemes

Scheme	Steps	Barrier	Strike	Abs. Error	Rel. Error	Time (s)
LOG_EULER-D	360	110.00%	90.00%	45,273	0.40%	43.9
LOG_EULER-S	180	110.00%	90.00%	1,338	0.01%	29.0
LOG_EULER-S	90	110.00%	90.00%	36,766	0.32%	18.3
LOG_EULER-S	22	110.00%	90.00%	370,583	3.27%	10.2
LOG_EULER-D	360	130.00%	90.00%	49,659	0.08%	43.5
LOG_EULER-S	180	130.00%	90.00%	55,703	0.09%	30.1
LOG_EULER-S	90	130.00%	90.00%	75,354	0.12%	19.0
LOG_EULER-S	22	130.00%	90.00%	181,280	0.28%	10.3
LOG_EULER-D	360	110.00%	70.00%	83,224	0.09%	43.7
LOG_EULER-S	180	110.00%	70.00%	60,553	0.07%	29.1
LOG_EULER-S	90	110.00%	70.00%	207,720	0.23%	18.5
LOG_EULER-S	22	110.00%	70.00%	1,334,750	1.46%	9.9

The barrier adjustment does not result in any real loss of precision when the number of simulation dates is divided by 2, and has a relatively low error when the number of dates is divided by 4, which corresponds to a 2x speedup in practice (Table 2).

8. A FINITE DIFFERENCE IMPLEMENTATION

8.1. **Backward Evaluation.** Let's look at how to find an accurate price the Accumulator described in Table 1. We will note S the simulated asset, K the strike, B the knock-out barrier level, Q the total number of accumulated shares and V the option value.

We have presented a forward evaluation pseudo-code in Listing 1 for the Monte-Carlo simulation. Listing 2 presents an equivalent backward evaluation pseudo-code, used in a finite difference discretization of the local volatility PDE. Similarly to the discretely sampled asian option studied in [Wilmott et al., 2000], it relies on the definition of an extra variable Q representing the total number of accumulated shares. The continuity condition around accrual dates is:

$$V(t_i^-, S, Q) = V(t_i^+, S, Q + q) \tag{26}$$

where $q = 600$ for $S < K$ and else $q = 1200$. As the accumulated number of shares is reset to 0, the continuity condition around payment dates is:

$$V(t_i^-, S, Q) = V(t_i^+, S, 0) + Q(S - K) \tag{27}$$

And if there is a knock-out, that is when the asset price is higher than the barrier, it becomes simply:

$$V(t_i^-, S, Q) = Q(S - K) \tag{28}$$

The standard implementation of the extra variable continuity conditions is to use a quadratic or cubic spline interpolation [Tavella and Randall, 2000] on a discretization of this variable potential values with a predefined number of discretization steps. A nice property of the Accumulator, is that it is linear in Q, that means that we can reduce the discretization of the Q variable and rely on linear extrapolation, and as a result, improve the pricing time significantly.

LISTING 2. Backward evaluation pseudo-code

```
PaymentDates:
  Value(S,Q) = Value(S,0) + Q*(S–K)

KnockoutDates:
  if S >= B then
    Value(S,Q) = Q*(S–K)
  endif

AccrualDates:
  q = S > K ? 1200 : 600
  Value(S,Q) = Value(S,Q+q)
```

8.2. **The Grid.** One has to be careful to place the barrier in the middle of the finite difference grid in order to have good convergence without using too fine a discretization [Tavella and Randall, 2000]. One solution is to use a nearly uniform transform based on cubic spline as described in [Tavella and Randall, 2000] to place the barrier in the middle of two grid points and the strike on the grid. This can be combined with a hyperbolic sine transformation that concentrates the points around the barrier to further reduce the total number of grid points needed:

$$S_i = B + \alpha \sinh(c_2 u_i + c_1(1 - u_i)) \tag{29}$$

with $c_1 = \text{asinh}(\frac{1}{\alpha}(S_{min} - B))$, $c_2 = \text{asinh}(\frac{1}{\alpha}(S_{max} - B))$ and u_i a uniform discretization of [0,1].

The spline construction can also be directly used to concentrate points. Two additional points P_i^- and P_i^+ are added around each point P_i where higher density is needed. Two parameters control how those points are placed: a width w corresponding to the distance between those points, and a slope $s \in (0, 1]$ corresponding to the slope of the line passing through the 3 points. $s \ll 1$ will lead to a high concentration, $s \approx 1$ will lead to a nearly uniform grid. w will control how far the

region of concentrated points extends. Outside of the concentrated part, the grid will be nearly uniform. Let n be the number of points, $d = (S_{max} - S_{min})/n$,. The associated point P_i' to P_i is defined as:

$$P_i' = S_{min} + d\,\text{round}(\frac{P_i - S_{min}}{d}) + \gamma\frac{d}{2} \tag{30}$$

where $\gamma = 0$ to place P_i on the grid and $\gamma = 1$ to place P_i in the middle. The spline transformation f is characterized by the following points:

$$\begin{aligned} f(P_i^-) = f(P_i' - w) &= P_i - ws \\ f(P'i) &= P_i \\ f(P_i^+) = f(P'i + w) &= P_i + ws \end{aligned}$$

and $f(S_{min}) = S_{min}$, $f(S_{max}) = S_{max}$. We use a monotonic spline [Dougherty et al., 1989] as a standard cubic spline is not guaranteed to preserve monotonicity.

FIGURE 19. Non-uniform grids with 31 points used on the daily Accumulator with $\alpha = 0.01(S_{max} - S_{min})$, $w = 0.05 \cdot S(0)$, $s = 0.1$.

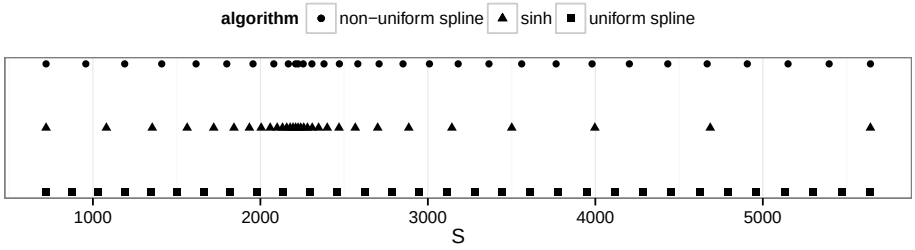

The advantage of such a transform is that it can be used to increase the density around a set of points, separately, typically for derivatives with more than 1 barrier. Furthermore the parameters have a nice intuitive geometrical explanation.

8.3. **Results.** Another important aspect is the choice of finite difference scheme: we use TR-BDF2. As it is L-stable (while the Crank-Nicolson is only A-stable) it will smooth out the discontinuities, just like implicit Euler, while keeping a higher order of convergence [Le Floc'h, 2013]. This is especially important on highly non-uniform grids where Crank-Nicolson is known to strongly oscillate.

We found that we already achieved a very good performance with the nearly uniform grid: a 1000 by 1000 grid gave a relative error of 10^{-3}. The hyperbolic sine transform with $\alpha = 0.01(S_{max} - S_{min})$ allowed to gain an order of magnitude in precision. The non-uniform spline tranformation improved precision even more especially when the number of space-steps is low with $w = 0.05S(0)$, $s = 0.1$ (see Table 3).

The time to price the Accumulator was less than 0.4s on a grid of 1000 time-steps and 500 space-steps using the TR-BDF2 finite-difference scheme, 100 times faster than a Monte-Carlo Euler simulation over 512K paths. It also achieves a much higher accuracy: 10^{-4} compared to $5 \cdot 10^{-3}$.

8.4. **The Greeks.** Let's now look at how stable are the greeks. This is of critical importance as those are usually directly used for hedging. We compute the Delta

TABLE 3. Daily Accumulator price under Dupire local volatility computed with the TR-BDF2 finite difference scheme on a non-uniform grid

Space Steps	Time Steps	Price	Rel. Error	Time (s)
62	500	11,268,593	-5.92E-03	0.09
125	500	11,363,450	2.45E-03	0.11
250	500	11,334,140	-1.37E-04	0.18
500	1000	11,335,364	-2.93E-05	0.46
2000	8000	11,334,740	-8.43E-05	7.61

and Gamma greeks numerically by centered finite difference, not to be confused with our finite difference partial differential equation solver:

$$\Delta = \frac{V(S+\epsilon) - V(S-\epsilon)}{2\epsilon} \tag{31}$$

$$\Gamma = \frac{V(S+\epsilon) - 2V(S) + V(S-\epsilon)}{\epsilon^2} \tag{32}$$

where $\epsilon = 10^{-2}S$ and V is the price obtained by Monte-Carlo simulation with a given discretization or by Finite Difference.

The finite difference grid gives directly access to another Delta measure. While it coincides with the numerical Δ when the volatility is flat, it is different in the general case. The local volatility depends on the current forward value, and therefore on the initial spot used. The finite difference grid Delta includes a static local volatility effect (the local volatility is different at each grid point), but in reality the local volatility surface is not static: when the spot moves, the whole surface changes. This dynamic will be included in the numerical Δ.

FIGURE 20. Greeks for the daily accumulator using 128K paths

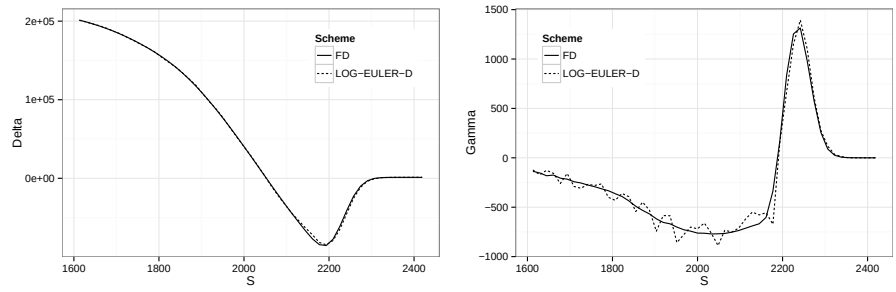

(A) Δ (B) Γ

Figure 20 shows how stable is the Γ resulting from our finite difference implementation (labeled "FD") on the daily Accumulator under Dupire local volatility model. In contrast, the Monte-Carlo Γ has many wiggles, directly related to the variance of the computed price. Possible solutions are to use more paths, or alternatively to switch to the likelyhood-ratio method known to work better on discontinuous payoffs. When ϵ is smaller, the wiggles are more pronounced and can appear in the Δ as well. With a really small ϵ, the finite difference solution will also have wiggles, this is more pronounced on non-uniform grids than on uniform grids, as well as if the grid is different for every computation of V. Our choice of ϵ is often used in practice to produce risk reports.

9. Conclusion

Under the displaced diffusion model, Standard and log discretizations have different convergence. The Milstein scheme offers better convergence on discontinuous payoffs that are sampled relatively rarely (monthly), the log-Milstein discretization does not when compared to the simpler Euler or log-Euler discretizations. The predictor-corrector schemes, while they are an improvement over Euler or log-Euler, are not an improvement over Milstein and have the disadvantage of being the slowest. When the payoff requires evaluation very frequently, like the daily Accumulator, all the discretizations have a similar convergence, and Euler would therefore be the most efficient. We also note that the exponential function evaluation can present a significant overhead even on the evaluation of relatively complex payoffs like the accumulator, and therefore when the time step size is small, Euler is much more efficient than log-Euler in those cases.

Under the Dupire model, the direct use in the Monte-Carlo simulation of the resulting discrete local volatility is a simple way to improve the accuracy, preferable to more costly alternatives. Furthermore, the Milstein scheme improvements in convergence are less obvious, and the standard Euler scheme has better convergence overall than the log-Euler scheme. Barrier shifting techniques allow to speed up slightly the pricing of the Accumulator by Monte-Carlo simulation, under displaced diffusion as well as under Dupire local volatility.

Finally, the finite difference method is particularly attractive to price the Accumulator under local volatility: it is much faster, more accurate and gives smooth greeks with the TR-BDF2 scheme.

References

Andersen, L. and Andreasen, J. (2000). Volatility skews and extensions of the libor market model. *Applied Mathematical Finance*, 7(1):1–32.

Andersen, L. and Brotherton-Ratcliffe, R. (1998). The equity option volatility smile: a finite difference approach. *Journal of Computational Finance*, 1(2):5–38.

Andersen, L. and Piterbarg, V. (2010). Interest rate modeling, volume i: Foundations and vanilla models.

Broadie, M., Glasserman, P., and Kou, S. (1997). A continuity correction for discrete barrier options. *Mathematical Finance*, 7(4):325–349.

Clark, I. (2011). *Foreign Exchange Option Pricing: A Practitioners Guide*. Wiley.

Dougherty, R., Edelman, A., and Hyman, J. (1989). Nonnegativity-, monotonicity-, or convexity-preserving cubic and quintic hermite interpolation. *Mathematics of Computation*, 52(186):471–494.

Dupire, B. (1994). Pricing with a smile. *Risk*, 7(1):18–20.

Gatheral, J. (2006). *The volatility surface: a practitioner's guide*, volume 357. Wiley.

Glasserman, P. (2003). *Monte-Carlo Methods in Financial Engineering*. Springer.

Gobet, E. (2008). Advanced monte carlo methods for barrier and related exotic options. *Mathematical Modelling and Numerical Methods in Finance*.

Haug, E. G. (2006). *The complete guide to option pricing formulas*. McGraw-Hill, New York, 2nd. edition.

Jäckel, P. (2002). *Monte Carlo methods in finance*. J. Wiley.

Joe, S. and Kuo, F. (2008). Constructing sobol sequences with better two-dimensional projections. *SIAM Journal on Scientific Computing*, 30(5):2635–2654.

Kou, S. (2003). On pricing of discrete barrier options. *Statistica Sinica*, 13(4):955–964.

Lam, K., Yu, P., and Xin, L. (2009). Accumulator pricing. In *Computational Intelligence for Financial Engineering, 2009. CIFEr'09. IEEE Symposium on*, pages 72–79. IEEE.

Le Floc'h, F. (2013). Tr-bdf2 for stable american option pricing. *Journal of Computational Finance*.

Rubinstein, M. (1983). Displaced diffusion option pricing. *The Journal of Finance*, 38(1):213–217.

Santini, L. (2009). Accumulators are collecting fans again. *The Wall Street Journal*.

Taleb, N. (1997). *Dynamic hedging: Managing vanilla and exotic options*, volume 64. Wiley.

Tavella, D. and Randall, C. (2000). *Pricing financial instruments: The finite difference method*. New York: John Wiley & Sons.

Wilmott, P., Dewynne, J., and Howison, S. (2000). *Option Pricing: Mathematical Models and Computation*. Oxford financial press.

Calypso Technology, 106 rue de La Boétie, Paris
E-mail address: fabien_lefloch@calypso.com
URL: www.calypso.com